

SYNTHESIS, CHARACTERIZATION AND THERMAL STUDIES OF SOME IRON(III) COMPLEXES OF *o*-VANILLIN OXIME

M. R. P. Kurup¹, E. Lukose² and K. Muraleedharan¹

¹Department of Applied Chemistry, Cochin University of Science and Technology, Kochi 682 022

²Department of Chemistry, St. Joseph's College for Women, Alappuzha 688 001, India

(Received July 3, 1999)

Abstract

Iron(III) complexes of *o*-vanillin oxime have been synthesized and characterized by different physicochemical techniques. The complexes containing thiocyanate, iodide and sulphate ions have been subjected to non-isothermal decomposition studies in N₂ using TG and DTG techniques. The kinetic parameters for both stages of decomposition of these complexes were evaluated by weighted least-squares method using the general approach as well as the Coats-Redfern and Horowitz-Metzger equations. The results indicate that the values of kinetic parameters obtained by these three different approaches agree well.

Keywords: iron(III) complex, kinetic parameters, non-isothermal decomposition, *o*-vanillin oxime

Introduction

Owing to the diverse applications of coordination compounds in chemistry and technology, there exists continuing interest in the synthesis and characterization of compounds especially those of 3d-transition metals. Coordination chemistries of transition metals with hydroxyloxime find applications as analytical reagents in solvent extraction systems [1–3] and in hydrometallurgy [4–6]. As a part of our investigations on the synthesis, characterization and thermal behaviour and kinetics of decomposition of transition metal complexes [7–9], we report here the synthesis, spectral and thermal studies of some iron(III) complexes of *o*-vanillin oxime.

Experimental

All chemicals used were of BDH AnalaR grade. The ligand *o*-vanillin oxime (HL) (Fig. 1) was prepared by the reported method [10].

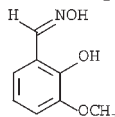


Fig. 1 Structure of *o*-vanillin oxime, HL

Preparation of complexes

The iron(III) complex with thiocyanate anion is prepared by refluxing a mixture of ferric nitrate, ammonium thiocyanate and *o*-vanillin oxime in the molar ratio of 1:1:2 in methanol for about one h in a hot water bath. In the case of complex with iodide ion, the procedure is the same, but potassium iodide is used instead of ammonium thiocyanate. All other complexes were prepared by refluxing a methanolic solution of the metal salt and the ligand in the molar ratio of 1:2 for about one h. The crystalline complexes formed on cooling were filtered, washed, recrystallized from methanol and dried over P_4O_{10} in vacuo.

Physical measurements

C, H and N microanalyses are conducted on a Perkin Elmer Elemental Analyzer. Iron in the complex was estimated gravimetrically as iron oxide [11]. Magnetic measurements were carried out at 300 ± 1 K on Gouy balance, using $Hg[Co(CNS)_4]$ as calibrant. Molar conductance were measured in DMF as well as in MeOH at 300 ± 1 K using a Systronic model digital conductivity meter. The molecular mass were determined in dichloromethane at 300 K on a Mechrolab vapour phase osmometer. Electronic spectra in 2-propanol were recorded on a Shimadzu model uv-240. The 1H NMR spectrum of ligand was recorded in $CDCl_3$ using Hitachi R-600 AFT NMR spectrophotometer. IR spectra were recorded in the range $4600-400\text{ cm}^{-1}$ on Shimadzu HAPP Genzel spectrophotometer in KBr disc. Thermal analyses were conducted on a Perkin Elmer Analyzer with the following operational characteristics. Heating rate, 10 K min^{-1} ; sample size, 6–10 mg; atmosphere, nitrogen flowing at a rate of $40\text{ cm}^3\text{ min}^{-1}$; crucible, platinum.

Results and discussion

Stereochemical investigations

The colours, elemental analyses and stoichiometries of HL, and its complexes are presented in Table 1. All the complexes are soluble in methanol, isopropanol, DMF, DMSO, nitrobenzene and chloroform. The elemental analyses results of the complexes correspond to the general formulae, $[FeL_2(H_2O)_2]X$, where $X=Cl, NO_3, CH_3COO, I$ or NCS and $[FeL_2H_2O]_2SO_4$. The molar conductance values obtained are found to be consistent with 1:1 electrolytic nature of the complexes, except $[FeL_2H_2O]_2SO_4$ which is found to be a 2:1 electrolyte in agreement with the molecular formulae. The ionic nature of all complexes is corroborate by molecular mass determination in dichloromethane.

The magnetic susceptibility values of these complexes are in the range 1.8 to $2.5\ \mu B$ which indicate the presence of one unpaired electron. The significant electronic absorption bands for the complexes recorded in solution are presented in Table 2.

Table 1 Colours, elemental analyses, molar conductance and magnetic susceptibility data

Compound	Colour	Elemental analysis/% found (calcd.)				Molar conductance ^a / ohm ⁻¹ cm ² mol ⁻¹	Magnetic susceptibility/ μB
		C	H	N	Fe		
HL		57.1 (57.4)	5.7 (5.4)	8.6 (8.4)			
[FeL ₂ (H ₂ O) ₂]NCS	reddish brown	41.8 (42.3)	4.0 (4.2)	8.1 (8.7)	11.4 (11.3)	79 (92)	2.49
[FeL ₂ (H ₂ O) ₂]I	deep brown	35.1 (34.8)	3.8 (3.6)	5.6 (5.0)	10.0 (10.1)	84 (101)	2.40
[FeL ₂ (H ₂ O) ₂]SO ₄	greenish brown	42.8 (42.3)	3.1 (3.9)	5.7 (6.1)	12.0 (12.1)	110 (130)	2.20 ^b
[FeL ₂ (H ₂ O) ₂]Cl	violet	42.0 (41.8)	4.7 (4.3)	6.3 (6.1)	11.8 (12.2)	82 (86)	1.89
[FeL ₂ (H ₂ O) ₂]OOCCH ₃	brown	45.4 (44.7)	4.4 (4.7)	6.1 (5.8)	10.9 (11.5)	69 (82)	2.16
[FeL ₂ (H ₂ O) ₂]NO ₃	greenish black	39.2 (39.5)	4.2 (4.1)	9.0 (8.6)	11.6 (11.5)	75 (95)	1.96

^a ca 10⁻³ M DMF solution (ca 10⁻³ M MeOH solution); ^b Magnetic susceptibility per Fe(III)

Table 2 Electronic spectral data

Compound	Absorption maxima/cm ⁻¹ (ϵ in parenthesis)		
	intra ligand bands	charge transfer bands	d-d bands
HL	38160 (50190)	31650 (49490)	
[FeL ₂ (H ₂ O) ₂]NCS	38120 (52310)	32020 (51300)	20830 (640)
[FeL ₂ (H ₂ O) ₂]I	38130 (52400)	31350 (51220)	21740 (580)
[FeL ₂ (H ₂ O) ₂]SO ₄	38540 (52100)	31770 (51310)	20410 (590)
[FeL ₂ (H ₂ O) ₂]Cl	38210 (52490)	31650 (50890)	21440 (610)
[FeL ₂ (H ₂ O) ₂]OOCCH ₃	38420 (52210)	31390 (50890)	20700 (605)
[FeL ₂ (H ₂ O) ₂]NO ₃	38410 (52400)	31430 (51410)	21310 (595)

The oxime has two intense bands at 38160 and 31650 cm⁻¹ which are assigned to ring $\pi \rightarrow \pi^*$ and $n \rightarrow \pi^*$ respectively. All the complexes are also dominated by these two bands. For the complexes a band situated around 32000 cm⁻¹ is assigned to a combination of intraligand and ligand to metal charge transfer bands. There is another shoulder band of less intensity around 22000 cm⁻¹ corresponds to a combination of ${}^6A_{1g} \rightarrow {}^4T_{1g}$, ${}^6A_{1g} \rightarrow {}^4T_{2g}$, ${}^6A_{1g} \rightarrow {}^4E_g$ forbidden transitions is the octahedral symmetry [12].

Table 3 Infrared band assignments of the oxime and its iron(III) complexes*

Compound	Absorption maxima/cm ⁻¹					
	$\nu(\text{O-H})$	$\nu(\text{C=N})$	$\nu(\text{C-O})$	$\nu(\text{N-O})$	$\nu(\text{Fe-N})$	$\nu(\text{Fe-O})$
HL	3300 s	1650 m	1510 m	963 s		
[FeL ₂ (H ₂ O) ₂]NCS ^{a,b}	3380 s	1625 w	1540 m	995 s	550 sh	425 sh
[FeL ₂ (H ₂ O) ₂] ^b	3350 s	1630 m	1560 s	997 s	570 m	430 m
[FeL ₂ (H ₂ O) ₂]SO ₄ ^{b,c}	3350 s	1622 m	1530 m	995 s	530 sh	430 m
[FeL ₂ (H ₂ O) ₂]Cl ^b	3350 s	1640 m	1560 s	1002 s	540 m	420 m
[FeL ₂ (H ₂ O) ₂]OOCCH ₃ ^{b,d}	3334 s	1620 w	1540 m	997 m	570 w	425 m
[FeL ₂ (H ₂ O) ₂]NO ₃ ^{b,c}	3340 s	1635 m	1550 s	992 s	540 m	415 m

*s=strong, m=medium, w=weak, sh=shoulder, ^a $\nu(\text{CN})$ 2058 s of the thiocyanate group, ^b $\nu(\text{OH})$ 3020–3040, $\nu(\text{H}_2\text{O})$ 839 cm⁻¹ of H₂O, ^c ν_3 1092 vs of the sulphate group, ^d $\nu(\text{COO})$ 1418 s, $\nu(\text{COO})$ 1579 s of acetate group and ^e $\nu_1 + \nu_4 = 1752$ w of nitrate group

Infrared spectral bands of the ligand and its complexes with the tentative assignments are presented in Table 3. The band at 3300 cm⁻¹ of high intensity in the case of free ligand implies that the hydroxyl group of the oxime is engaged in an intermolecular hydrogen bond [13]. The medium band at 1650 cm⁻¹ of the ligand is assigned to $\nu\text{C=N}$ and this band is shifted to lower wave numbers indicating the coordination of oxime nitrogen in all complexes [14–16]. The coordination of phenolic group is indicated by the positive shift of $\nu(\text{C-O})$ band at 1510 cm⁻¹. The band seen at 962 cm⁻¹ corresponding to $\nu\text{N-O}$ of

Table 4 Thermal decomposition data

Compound	Decomposition stage	DTG peak temperature/ K	Decomposition temperature range/ K	Mass loss from TG/% (theoretical)	Leaving group	Metal residue from TG/% (theoretical)
[FeL ₂ (H ₂ O) ₂]NCS	1	553	360–660	54.0 (54.2)	2H ₂ O, 1L, 1HCNS	
	2	724	660–760	34.2 (34.5)	1L	11.4 (11.3)
[FeL ₂ (H ₂ O) ₂]I	1	512	360–600	37.0 (36.7)	2H ₂ O, 1L	
	2	844	640–960	53.0 (53.2)	1L, 1HI	10.0 (10.1)
[FeL ₂ (H ₂ O) ₂]SO ₄	1	499	380–570	67.6 (67.4)	3L, 1H ₂ O, 1H ₂ SO ₄	
	2	724	640–780	20.3 (20.5)	1L, 1H ₂ O	12.0 (12.1)

the free ligand [17, 18] is shifted to higher wave numbers indicating the coordination of metal ion through nitrogen atom of the oxime.

All the complexes show a band in the region 3330–3380 cm^{-1} due to the $\nu\text{O-H}$ of the water molecule [19]. A double hump at 3020–3040 cm^{-1} and a sharp band at 839 cm^{-1} are also seen in the spectra of the complexes which are due to the presence of coordinated water molecule [20]. The bands around 550 and 425 cm^{-1} are assigned to the $\nu\text{Fe-N}$ and $\nu\text{Fe-O}$ vibrations. The nitrate complex shows a strong band at 1092 cm^{-1} and a weak band at 650 cm^{-1} . The acetate complex shows bands at 1579 and 1418 cm^{-1} and thiocyanate complex shows a band at 2058 cm^{-1} indicating the ionic nature of the anions [21].

Thermal decomposition studies

We have studied the thermal decomposition and kinetics of three of these, viz., thiocyanate, iodide, and sulphate complexes. The general thermal behaviours of these complexes, their stability ranges, DTG peak temperatures and mass loss data are given in Table 4. Thermal studies show that all the complexes decompose in two stages. The thiocyanate complex, $[\text{FeL}_2(\text{H}_2\text{O})_2]\text{NCS}$ first decomposes in the temperature range 360–660 K eliminating two molecules of water, one molecule each of ligand and HCNS. The theoretical mass loss of 54.2% for this change agrees very well with the observed mass loss of 54%. In the second stage (660–750 K), the mass loss of 34.2% observed corresponds to the loss of one molecule of ligand. Similarly, $[\text{FeL}_2(\text{H}_2\text{O})_2]\text{I}$ decomposes in two steps. The first stage (360–600 K) corresponds to the loss of two molecules of water and one molecule of ligand. In the second stage (640–960 K), one molecule each of the ligand and HI are eliminated. The complex, $[\text{FeL}_2\text{H}_2\text{O}]_2\text{SO}_4$ also shows two stages of decomposition. In this case, three molecules of ligand, one molecule each of water and H_2SO_4 is lost in the temperature range 380–570 K. The second molecule of water is eliminated in the second stage (640–780 K) along with one molecule of ligand. The theoretical and observed mass losses for both stages of decomposition of all these complexes agree very well (Table 4). The residue of the decomposition is found to be metallic iron in all cases.

Decomposition kinetics

In recent years, there has been increasing interest in determining the rate dependent parameters of solid-state non-isothermal decomposition reactions from an analysis of the thermogravimetric (TG) curve. Several authors [22–30] discussed the advantages of this method over the conventional isothermal method. The rate of a decomposition process under non-isothermal conditions can be described [22] as the product of two separate functions of temperature and conversion as

$$d\alpha/dt = k(T)f(\alpha) \quad (1)$$

where the function $k(T)$ is temperature dependent and $f(\alpha)$ is the conversion function dependent on the mechanism of the reaction. It has been shown [29–32] that the tempera-

ture dependent function $k(T)$ is of the Arrhenius type and can be considered as the rate constant k :

$$k = Ae^{-E/RT} \quad (2)$$

where A is the pre-exponential factor, E is the activation energy and R is the gas constant. Combining Eqs (1) and (2) we obtain

$$d\alpha/f(\alpha) = (A/q)e^{-E/RT} dT \quad (3)$$

where q is the linear heating rate, dT/dt . Equation (3) on integration and taking logarithms yields

$$\ln g(\alpha) = \ln[AF/qR] + \ln p(x) \quad (4)$$

where $p(x) = \int_x^{\infty} e^{-x}/x^2$ and $x=E/RT$

Table 5 Mechanistic equations for solid state reactions

Function	Equation [$g(\alpha)=kt$]	Rate controlling process
D1	$\alpha^2=kt$	one-dimensional diffusion
D2	$(1-\alpha)\ln(1-\alpha)+\alpha=kt$	two-dimensional diffusion, cylindrical symmetry
D3	$[1-(1-\alpha)^{1/3}]^2=kt$	three-dimensional diffusion, spherical symmetry, Jander equation
D4	$(1-(2\alpha/3)-(1-\alpha)^{2/3})=kt$	three-dimensional diffusion, spherical symmetry, Ginstling-Brounshtein equation
R2	$1-(1-\alpha)^{1/2}=kt$	phase boundary reaction, cylindrical symmetry
R3	$1-(1-\alpha)^{1/3}=kt$	phase boundary reaction, spherical symmetry
F1	$-\ln(1-\alpha)=kt$	random nucleation, one nucleus on each particle Mampel equation
A2,A3 or A4	$-\ln(1-\alpha)^{1/n}=kt$ $n=2, 3$ or 4	random nucleation, ingestion and overlap of growth nuclei, Avrami-Erofe'ev equation

This is the basic form of the equation used for analysing non-isothermal data. This equation can be readily applied once the form of the function $p(x)$ is established. It has been shown [32, 33] that $\ln p(x)$ is, to a first approximation, a linear function of $1/T$. It is thus evident from Eq. (4) that $\ln g(\alpha)$ must also be a linear function of $1/T$ since $\ln[AE/qR]$ is independent of temperature. This fact opens up a method for estimating the most probable reaction path from a single non-isotherm. A plot of $g(\alpha)$ vs. $1/T$ must be a straight line for the correct mechanism and non-linear for an incorrect mechanism. Thus, by calculating the values of $\ln g(\alpha)$ using a non-isothermal TG trace for the various rate processes in Table 5 and plotting term vs. $1/T$, the most probable mechanism corresponding to the linear plot can be determined.

Besides this general approach, several equation [22–24] are available in the literature for the analysis of a non-isothermal TG trace and for obtaining values of kinetic parameters. Most of them utilize Eq. (4) in three different approaches, namely integral, differential and approximation methods. The most accurate among them is the integral method [22, 34].

Integral methods are simpler because they do not involve the determination of rates even though they are complicated by the integration of the rate constant. Coats and Redfern [25] used the approximation for the $p(x)$ function as $\exp(-x)[1/x-2/x^2]$ and obtained

$$\ln[g(\alpha)/T^2] = \ln[(AR/qE)(1-2RT/E)] - E/RT \quad (5)$$

The first term on the right hand side of Eq. (5) is a slowly changing function of the temperature and may be considered as constant in a narrow temperature range [22]. Hence a plot of $\ln[g(\alpha)/T^2]$ vs. $1/T$ gives a straight line for the correct model relation, $g(\alpha)$.

Horowitz and Metzger [24] simplified the exponential integral with an approximation by defining a characteristic temperature deviation, θ , such that $T=T_s+\theta$, where T_s is the DTG peak temperature. After substituting this into Eq. (3), these authors derived the following equations

$$\ln[1-(1-\alpha)^{1-n}] = -E\theta/RT_s^2 + \ln(1-n) \text{ for } n \neq 1 \quad (6)$$

and

$$\ln[-\ln(1-\alpha)] = -E\theta/RT_s^2 + C \text{ for } n=1 \quad (7)$$

where C is a constant.

Evaluation of kinetic parameters

The TG curves for the three complexes are shown in Fig. 2. The instrumental TG curves were redrawn as curves of the fraction decomposed, α , vs. temperature, T , to obtain primary α - T data. All the complexes decompose in two stages. The decomposition reactions were subjected to non-isothermal kinetic investigations and the parameters such as E , A , activation entropy, ΔS , and the order parameter, n was evaluated. The linearity of an appropriate plot was assessed by means of the correlation

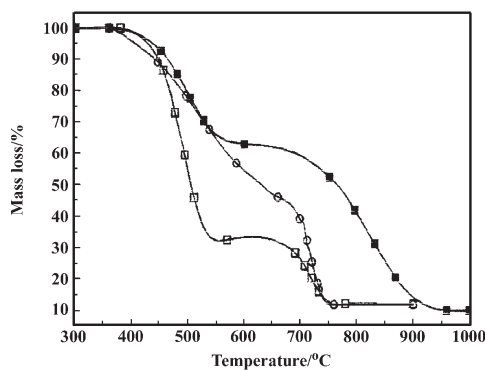


Fig. 2 TG curves of the complexes, o - $[\text{FeL}_2(\text{H}_2\text{O})_2]\text{NCS}$, ■ - $[\text{FeL}_2(\text{H}_2\text{O})_2]\text{I}$ and □ - $[\text{FeL}_2\text{H}_2\text{O})_2]\text{SO}_4$

Table 6 Kinetic parameters obtained by general approach (Fl) and the Coats-Redfern (CR) and Horowitz-Metzger (HM) methods

Complex	Eq.	First stage of decomposition				Second stage of decomposition			
		$E/\text{kJ mol}^{-1}$	$\ln A/\text{s}^{-1}$	$\Delta S/\text{J K}^{-1} \text{mol}^{-1}$	r	$E/\text{kJ mol}^{-1}$	$\ln A/\text{s}^{-1}$	$\Delta S/\text{J K}^{-1} \text{mol}^{-1}$	r
[FeL ₂ (H ₂ O) ₂]NCS	Fl	30.73	17.30	-1.20	-0.9999	268.83	57.42	334.52	-0.9994
	CR	22.17	2.48	-124.42	-0.9997	256.87	42.21	208.16	-0.9991
	HM	34.59	5.53	-99.07	0.9956	286.02	47.03	248.20	0.9994
[FeL ₂ (H ₂ O) ₂]I	Fl	51.22	23.17	46.90	-0.9999	91.48	24.75	64.20	-0.9999
	CR	43.06	8.59	-74.22	-0.9999	77.98	9.18	-65.17	-0.9999
	HM	55.30	11.62	-49.07	0.9993	98.23	12.20	-40.07	0.9976
[FeL ₂ (H ₂ O) ₂]SO ₄	Fl	69.59	28.20	88.51	-0.9999	199.50	45.62	236.49	-1.0000
	CR	61.59	13.70	-31.95	-0.9999	187.62	30.42	110.06	-0.9999
	HM	73.64	16.72	-6.91	0.9986	105.31	32.96	134.53	0.9999

coefficient, r , obtained by the weighted least-squares method (LSM). The masses used and other details are as reported in an earlier work [7, 30, 35].

The Freeman-Carroll equation [23] was used for the determination of the order of the reaction. But its applicability was found to be extremely poor as observed from the scattered plot. Several authors [36, 37] have made similar observations. Therefore, the method of Horowitz-Metzger [24] was applied and the order was determined by constructing a 'master curve' as reported elsewhere [38]. We also computed the values of r by using the weighted LSM, for the equations suggested by Coats and Redfern [25] (with $n=0, 1/2, 2/3$ and 1) and found a maximum value for the equation with $n=1$. Using this value of n , the kinetic parameters were evaluated separately for each stages of decomposition.

The different types of mechanism encountered most frequently in solid-state reactions are listed in Table 5. The weighted least-squares plot of all these functions vs. reciprocal absolute temperature was drawn for all the complexes and found that the F1 mechanism gives the best linear fit (with a maximum value of r) in all cases. Accordingly E was calculated from the slope and A was calculated from the intercept value as described in an earlier work [32]. ΔS was calculated using the following equation:

$$\Delta S = R \ln(Ah/kT_s) \quad (8)$$

where k is the Boltzmann constant and h is the Planck constant.

The kinetic parameters were also evaluated using the integral method of Coats and Redfern and the approximation method of Horowitz and Metzger.

The kinetic data obtained using the general approach, Coats-Redfern and Horowitz-Metzger methods are given in Table 6. The satisfactory values of r (≈ 1) in all cases indicate good agreement with the experimental data. The values of kinetic parameters obtained from these three different approaches are reasonable and in good agreement to some extent. The first stage decomposition of all these complexes is very slow. The second stage of decomposition in the case of thiocyanate and sulphate complex is very fast, and consequently it gives positive value for ΔS . Even though the second stage of decomposition of iodide complex was faster than the first stage, they still have negative values of ΔS , which indicates that, in both stages of decomposition, the activated complex has a more ordered structure than the reactants and that the reactions are slower than normal [30, 39]. A close examination of the results reveals that these complexes show similar thermal behaviour that is as expected given their similar structures.

* * *

One of us (K. M.) is thankful to Prof. M. P. Kannan, Department of Chemistry University of Calicut, Kerala, India for some helpful discussions.

References

- 1 M. E. Keeney, K. Osseo-Asare and K. A. Woods, *Coord. Chem. Rev.*, 59 (1984) 141.
- 2 A. Chakravorty, *Coord. Chem. Rev.*, 13 (1974) 1.

- 3 R. B. Singh, B. S. Garg and R. P. Singh, *Talanta*, 26 (1979) 425.
- 4 A. W. Ashbrook, *Coord. Chem. Rev.*, 16 (1975) 285.
- 5 J. S. Preston, *J. Inorg. Nucl. Chem.*, 37 (1975) 1235.
- 6 J. M. Pratt and R. I. Tilley, *Hydrometallurgy*, 5 (1979) 29.
- 7 K. K. Aravindakshan and K. Muraleedharan, *J. Thermal Anal.*, 37 (1991) 791.
- 8 K. K. Aravindakshan and K. Muraleedharan, *Thermochim. Acta*, 159 (1990) 101.
- 9 K. K. Aravindakshan and K. Muraleedharan, *J. Thermal Anal.*, 37 (1991) 803.
- 10 A. I. Vogel, *A Text Book of Practical Organic Chemistry*, 3rd Ed., Longmans, London 1973.
- 11 A. I. Vogel, *A Text Book of Quantitative Inorganic Analysis*, 4th Ed., Longmans, London 1978.
- 12 S. A. Cotton, *Coord. Chem. Rev.*, 8 (1972) 184.
- 13 R. M. Silverstein, G. C. Bassler and T. C. Morrill, *Spectroscopic Identification of Organic Compounds*, 5th Ed., Wiley, New York 1991.
- 14 N. K. Dutt and M. C. Chakder, *J. Inorg. Nucl. Chem.*, 32 (1970) 2303.
- 15 V. Coto, P. Souza, J. R. Masageur and A. Arquero, *Trans. Met. Chem.*, 11 (1986) 373.
- 16 R. Raina and T. S. Srivastava, *Inorg. Chim. Acta*, 67 (1982) 83.
- 17 A. Palm and H. Werbun, *Can. J. Chem.*, 32 (1954) 858.
- 18 R. E. Rundle and M. Parasal, *J. Chem. Phys.*, 4 (1965) 1382.
- 19 J. R. Ferraro and W. R. Wacker, *Inorg. Chem.*, 4 (1965) 1382.
- 20 T. Gamo, *Bull. Chem. Soc. Jpn.*, 34 (1961) 760.
- 21 L. J. Bellamy, *The Infrared Spectra of Complex Molecules*, Vol. I, Chapman & Hall, London 1986.
- 22 J. Šesták, V. Satava and W. W. Wendlandt, *Thermochim. Acta*, 7 (1973) 333.
- 23 E. S. Freeman and B. Carroll, *J. Phys. Chem.*, 62 (1958) 394.
- 24 H. Horowitz and G. Metzger, *Anal. Chem.*, 35 (1963) 1464.
- 25 A. W. Coats and J. P. Redfern, *Nature*, 201 (1964) 68.
- 26 W. W. Wendlandt, *Thermal Methods of Analysis*, Wiley, New York 1974.
- 27 T. Ozawa, *Bull. Chem. Soc. Jpn.*, 38 (1965) 1881.
- 28 J. H. Flynn and L. A. Wall, *Polym. Lett.*, 4 (1966) 323.
- 29 J. Šesták and G. Berggren, *Thermochim. Acta*, 3 (1971) 1.
- 30 K. K. Aravindakshan and K. Muraleedharan, *Reactivity of Solids*, 8 (1990) 91.
- 31 K. Krishnan, K. N. Ninan and P. M. Madhusudanan, *Thermochim. Acta*, 25 (1988) 111.
- 32 M. P. Kannan, K. Muraleedharan and T. Gangadevi, *Thermochim. Acta*, 86 (1991) 65.
- 33 J. Szako, *J. Thermal Anal.*, 2 (1970) 145.
- 34 J. Šesták, *Talanta*, 13 (1966) 567.
- 35 K. K. Aravindakshan and K. Muraleedharan, *Thermochim. Acta*, 140 (1989) 325.
- 36 R. L. Reed, L. Weber and B. S. Gottfried, *Ind. Eng. Chem. Fundament.*, 4 (1965) 38.
- 37 R. L. Bohn in H. G. McAdie (Ed.), *Proc. First Toronto Symposium on Thermal Analysis*, Chemical Institute of Canada, 1983.
- 38 P. M. Madhusudanan, P. N. K. Nambissan and C. G. R. Nair, *Thermochim. Acta*, 9 (1974) 149.
- 39 A. A. Frost and R. G. Pearson, *Kinetics and Mechanism*, Wiley, New York 1961.